Molecular Biology of the Cell
Vol. 10, 2033–2050, June 1999

Trafficking, Assembly, and Function of a Connexin43-Green Fluorescent Protein Chimera in Live Mammalian Cells[V]

Karen Jordan,* Joell L. Solan,† Michel Dominguez,‡§ Michael Sia,* Art Hand,‖ Paul D. Lampe,† and Dale W. Laird*¶

*Department of Anatomy and Cell Biology, University of Western Ontario, London, Ontario, Canada N6A 5C1; †Fred Hutchinson Cancer Research Center, Seattle, Washington, 98109; ‡Department of Anatomy and Cell Biology, McGill University, Montreal, Quebec, Canada H3A 2B2; and ‖Department of Pediatric Dentistry, School of Dental Medicine, University of Connecticut Health Center, Farmington, Connecticut 06030

Submitted September 23, 1998; Accepted March 15, 1999
Monitoring Editor: Mary C. Beckerle

To examine the trafficking, assembly, and turnover of connexin43 (Cx43) in living cells, we used an enhanced red-shifted mutant of green fluorescent protein (GFP) to construct a Cx43-GFP chimera. When cDNA encoding Cx43-GFP was transfected into communication-competent normal rat kidney cells, Cx43-negative Madin–Darby canine kidney (MDCK) cells, or communication-deficient Neuro2A or HeLa cells, the fusion protein of predicted length was expressed, transported, and assembled into gap junctions that exhibited the classical pentalaminar profile. Dye transfer studies showed that Cx43-GFP formed functional gap junction channels when transfected into otherwise communication-deficient HeLa or Neuro2A cells. Live imaging of Cx43-GFP in MDCK cells revealed that many gap junction plaques remained relatively immobile, whereas others coalesced laterally within the plasma membrane. Time-lapse imaging of live MDCK cells also revealed that Cx43-GFP was transported via highly mobile transport intermediates that could be divided into two size classes of <0.5 μm and 0.5–1.5 μm. In some cases, the larger intracellular Cx43-GFP transport intermediates were observed to form from the internalization of gap junctions, whereas the smaller transport intermediates may represent other routes of trafficking to or from the plasma membrane. The localization of Cx43-GFP in two transport compartments suggests that the dynamic formation and turnover of connexins may involve at least two distinct pathways.

INTRODUCTION

A gap junction channel is assembled when a hemichannel (connexon), composed of six connexins, traffics to the cell surface and docks with a hemichannel from a contacting cell (Bruzzone *et al.*, 1996; Laird 1996). These channels are typically found in tightly packed arrays often referred to as gap junction plaques (Goodenough *et al.*, 1996). Gap junctions allow for the intercellular passage of small molecules, including important secondary messengers (e.g., Ca^{2+}, inositol triphosphate, and cAMP) (Flagg-Newton and Loewenstein, 1979; Elfgang *et al.*, 1995). Most cells grown in culture and many tissues express the gap junction protein Cx43 (Goodenough *et al.*, 1996). Nevertheless, studies to date have been unable to examine the life cycle of Cx43 in living cells in real time. The relative interest in the mechanics and regulation of gap junction assembly and removal has increased recently as Cx43 and Cx37 have been shown to be essential for normal heart development (Reaume *et*

[V] Online version of this article contains video material for Figures 9–11. Online version available at www.molbiolcell.org.

§ Present Address: Mayo Clinic and Foundation, Rochester, MN, 55905.
¶ Corresponding author. E-mail address: dwlaird@julian.uwo.ca.

al., 1995) and female fertility (Simon *et al.*, 1997). In addition, connexin mutations have been linked or associated with inherited prelingual deafness (Kelsell *et al.*, 1997) and a form of Charcot-Marie-Tooth disease (Bergoffen *et al.*, 1993).

In recent years, green fluorescent protein (GFP) has been identified as a useful reporter protein (Chalfie *et al.*, 1994). The inherent fluorescent properties of GFP have made it an excellent fusion partner to study the trafficking, assembly, and secretion of both soluble and integral membrane proteins (Hanakam *et al.*, 1996; Yano *et al.*, 1997). Most proteins when fused to GFP retain their native targeting properties and traffic to the correct organelle (Naray-Fejes-Toth and Fejes-Toth 1996; Wang *et al.*, 1996; Pedraza *et al.*, 1997). A fusion of GFP and Tax-4 was used to examine the localization properties and function of this cyclic nucleotide gated channel (Komatsu *et al.*, 1996). The pH sensory protein (Hanakam *et al.* 1996) β2-adrenergic receptor (Barak *et al.*, 1997), major histocompatibility complex class II (Wubbolts *et al.*, 1996), and glucose transporter 4 (Dobson *et al.*, 1996) all were properly transported to the plasma membrane when fused to GFP. GFP fusion proteins have proven to be particularly informative in determining the nature of endoplasmic reticulum-to-Golgi transport (Presley *et al.*, 1997) and processes involved in protein secretion (Wacker *et al.*, 1997). To date, the trafficking and functional characteristics of a connexin-GFP fusion protein have not been characterized; however, when mRNA encoding a zebrafish connexin43.4 (Cx43.4)-GFP fusion protein was injected into a single-cell zebrafish embryos, structures resembling gap junctions were observed (Essner *et al.*, 1996).

The trafficking of a variety of integral membrane proteins from the site of biosynthesis in the endoplasmic reticulum to the plasma membrane has been intensely investigated. In our current study, we have generated a construct in which red-shifted GFP was fused to the carboxyl terminus of rat Cx43. Cx43-GFP was expressed in communication-competent and -incompetent mammalian cell lines. In all cases, Cx43-GFP was translated, transported to the plasma membrane, and assembled into gap junctions. Microinjection studies revealed that the fusion protein did not inhibit communication in communication-competent cells and was capable of assembling into functional gap junction channels in communication-deficient cell lines. Our time-lapse studies of living cells revealed Cx43-GFP within two populations of transport intermediates. The large transport intermediates were observed to form when pieces of gap junctions internalize. Once Cx43-GFP was delivered to the cell surface, it assembled into gap junction plaques that often coalesced within the plane of the cell membrane.

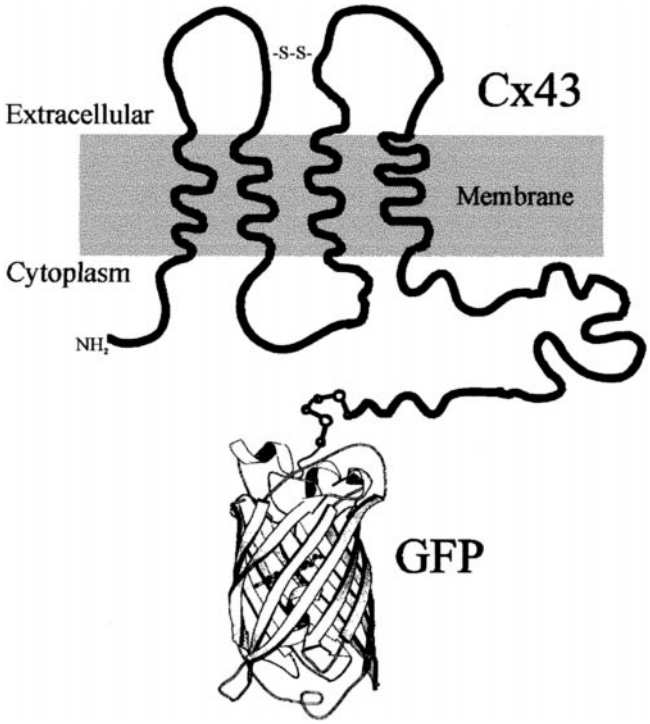

Figure 1. Schematic model of Cx43 traversing the membrane four times with GFP attached to the carboxyl terminal by a six-amino acid linker sequence. The drawing of the GFP moiety of the fusion protein was modified from Ormo *et al.* (1996).

MATERIALS AND METHODS

Engineering of Cx43-GFP Chimeric cDNA

Cx43 cDNA was PCR amplified from a Bluescript plasmid containing Cx43 (obtained from Dr. Eric Beyer, University of Chicago, Chicago, IL) using oligonucleotides GTGAAAGAGAGGTACCCAGAC to create a *Kpn*I site and GCCGGTTTAAGGATCCAGG to create a *Bam*HI site at the 5′ and 3′ ends of Cx43, respectively. PWO DNA polymerase (Boehringer Mannheim, Indianapolis, IN) was used for the reaction to ensure fidelity of the PCR reaction. PCR products and the vector pEGFP-N1 (Clontech, Palo Alto, CA) were digested with *Kpn*I and *Bam*HI, and the vector was dephosphorylated with alkaline phosphatase (Boehringer Mannheim). GFP was fused in frame to the carboxyl terminus of Cx43 with the addition of a six-amino acid polylinker (GATCCACCGGTCGCCACC) (Figure 1). After ligation, competent MC1069 *Escherichia coli* were transformed with the plasmid, and selected positive colonies were identified and digested with *Eco*RI and *Eco*RI–*Bam*HI restriction endonucleases. Finally, the cDNA encoding the chimeric protein was verified by the Applied Biosystems (Foster City, CA) dye terminator cycle sequencing method.

Cell Lines and Culture Conditions

All media, sera, and culture reagents were obtained from Life Technologies (Burlington, Ontario, Canada), Becton Dickinson (St. Laurent, Quebec, Canada) or Sigma (St. Louis, MO). LipofectAMINE was obtained from Life Technologies. Normal rat kidney (NRK), Madin–Darby canine kidney (MDCK), HeLa, and Neuro2A (N2A) cells were all grown in Dulbecco's modified Eagle's

medium supplemented with 10% FBS, 100 U/ml penicillin, 100 μg/ml streptomycin, and 2 mM glutamine.

Transfection of Mammalian Cells with cDNA Encoding Cx43-GFP

Mammalian cells grown to 50–75% confluency in 35- or 60-mm culture dishes were transfected in Opti-MEM1 medium (Life Technologies) containing LipofectAMINE and 1 μg of plasmid DNA (purified using a Qiagen [Hilden, Germany] Maxiprep column kit) for 5 h at 37°C. For transient transfections, the DNA/LipofectAMINE suspension was removed and replaced with culture medium. The efficiency of transfection was determined 24–48 h later by visualizing live or fixed cells under a fluorescence microscope. For selection of stably transfected MDCK, NRK, N2A, or HeLa cell lines, cells were trypsinized and plated at dilutions of 1:25 and 1:40 in the presence of 0.3–1.0 mg/ml G418. Selection media was changed every 3 d for 14–20 d. Individual colonies were selected with cloning cylinders, trypsinized, and expanded into clonal cell lines. Stably transfected cells were screened for Cx43-GFP expression by fluorescence microscopy.

Immunocytochemistry

Cells grown on coverslips were immunolabeled as previously described by Laird *et al.* (1995). Briefly, cells were grown on glass coverslips and fixed with 80% methanol and 20% acetone at −20°C or with 3.7% formaldehyde followed by 0.1% Triton X-100. Cells expressing Cx43-GFP were labeled with 1–5 μg/ml anti-Cx43 polyclonal antibody (Laird and Revel 1990), a 1:200 dilution of anti-Cx43 monoclonal antibody (Chemicon, Temecula, CA; specific for residues 252–270 of Cx43), a 1:500 dilution of a polyclonal antibody specific for the medial Golgi protein MG-160 (Gonatas *et al.*, 1989), or a 1:1000 dilution of anti-GFP polyclonal antibody (Clontech). Cells were washed six times over 30 min in PBS and incubated for 1 h in goat anti-mouse or donkey anti-rabbit antibodies conjugated to Texas Red (Jackson ImmunoResearch, West Grove, PA). Coverslips were rinsed in distilled water, mounted, and analyzed on a Zeiss (Thornwood, NY) LSM 410 inverted confocal microscope as described previously (Laird *et al.*, 1995).

Conventional and Immunoelectron Microscopy

For morphological studies, MDCK cells and MDCK cells that express Cx43-GFP were fixed for 1 h in 2.5% glutaraldehyde in 0.1 M cacodylate buffer, pH 7.2, gently scraped, and then pelleted at 1000 × *g* for 5 min. The pellets were resuspended and embedded in 3% agarose for easier handling. Cells within agarose blocks were washed several times with cacodylate buffer and postfixed with osmium-ferrocyanide (De Bruijn, 1973). After rinsing with distilled water and staining with 0.5% aqueous uranyl acetate, blocks were dehydrated in ascending concentrations of ethanol and embedded in Polybed epoxy resin (Polysciences, Warrington, PA). Thin sections were collected on 200-mesh copper grids and stained with uranyl acetate for 5 min, followed by lead citrate for 3 min. Electron micrographs were taken on a Philips (Mahwah, NJ) CM10 transmission electron microscope at 60 kV.

For immunolabeling studies, MDCK cells and MDCK cells that express Cx43-GFP were fixed for 1 h with cold 0.1% glutaraldehyde and fresh 3% paraformaldehyde in 0.1 M cacodylate buffer, pH 7.2. Cells were rinsed three times in 0.1 M cacodylate buffer containing 1% paraformaldehyde, scraped from the dish, and stored as a pellet. Blocks of cells immobilized in agarose were washed several times with cacodylate buffer, dehydrated in a graded series of methanol up to 90%, and then embedded in Lowicryl K4M (Polysciences) at −20°C. Sections were labeled with 20 μg/ml anti-Cx43 antibody (CT-360) or a 1:50–1:200 dilution of anti-GFP polyclonal antibody. The sections were blocked with 1% BSA and 1% nonfat dry milk in PBS for 30 min and then incubated with primary antibody diluted in 1% BSA and 5% normal goat serum overnight at 4°C followed by secondary goat anti-rabbit immunoglobulin G (IgG) conjugated to 10-nm gold particles (Amersham, Arllington Heights, IL) for 1 h at room temperature. Sections were stained with uranyl acetate and lead citrate and viewed as described above.

Microinjection

For Neurobiotin injections, clusters of three or more contacting HeLa or NRK cells that had been transiently transfected with the cDNA encoding Cx43-GFP were selected as sites of microinjection. One cell in each cluster was pressure microinjected with 2.5% Neurobiotin (Molecular Probes, Eugene, OR). In some cases, NRK cells stably expressing Cx43-GFP were microinjected with 2.7% Neurobiotin containing 4.5 mg/ml rat IgG to mark the injected cell. In all cases, transfer was allowed to proceed for 10–20 min, followed by fixation with 3.7% formaldehyde in PBS for 10 min, permeabilization with 0.1% Triton X-100, and labeling with streptavidin conjugated to Texas Red (Molecular Probes) and, in some cases, with goat anti-rat IgG conjugated to FITC. Cells were viewed under a microscope equipped for epifluorescence, and the percentage of microinjected cells that transferred Neurobiotin were scored. To be scored as positive, Neurobiotin was required to have transferred to two or more contacting cells. As controls, wild-type HeLa or NRK cells and HeLa or NRK cells transfected with the plasmid containing GFP only were microinjected as described above.

For Lucifer yellow dye transfer, one cell within a cluster of HeLa or N2A cells expressing Cx43-GFP was microinjected with 1% Lucifer yellow in 0.15 M LiCl until the cell was brightly fluorescent (usually a few seconds). After 5 min, the percentage of microinjected cells that transferred Lucifer yellow was determined. As controls, wild-type HeLa and N2A cells were microinjected with Lucifer yellow as described above.

Western Immunoblotting

HeLa cells, HeLa cells expressing GFP, HeLa cells expressing Cx43-GFP, or MDCK cells expressing Cx43-GFP were lysed in 2× Laemmli sample buffer containing protease inhibitors as previously described (Laird *et al.*, 1995). Lysates, together with recombinant GFP protein (Clontech), were resolved on a 10% SDS-polyacrylamide gel with a bisacrylamide:acrylamide ratio of 0.8:30 and transferred to nitrocellulose. Immunoblots were labeled with 1 μg/ml anti-Cx43 polyclonal antibody (specific for residues 2–21 of Cx43), 1:2000 diluted anti-Cx43 monoclonal antibody (Chemicon; specific for residues 252–270), or 1:2000 anti-GFP polyclonal antibody (Clontech). Finally, immunoblots were labeled with appropriate secondary antibodies conjugated to ^{125}I (ICN Biochemicals, Costa Mesa, CA). The blots were air dried and exposed to Amersham Hyperfilm-MP with an intensifying screen.

Imaging of Cx43-GFP in Living Cells

MDCK cells stably expressing Cx43-GFP were grown on 12-mm glass coverslips. Coverslips were inverted onto a glass-bottom 25-mm tissue culture dish, which contained 2 ml of Opti-MEM1 medium (Life Technologies) supplemented with 10 mM HEPES, pH 7.2. In some cases, live MDCK cells that express Cx43-GFP were treated with 1% Triton X-100 in situ, and images were collected before and after Triton X-100 treatment. Tissue culture dishes were placed on a 20/20 Technology (Mississauga, Ontario, Canada) temperature-controlled stage, and cells were maintained at 37°C for the duration of the experiment. Cells were imaged using a 488-nm argon/krypton laser line on a Zeiss LSM 410 inverted confocal microscope with a 63× oil (1.4 numerical aperture) objective. Optical scans were collected continuously at a scan speed of 32 s for periods up to 37.3 min The focus, contrast, or brightness settings remained constant during the course of image acquisition. For anal-

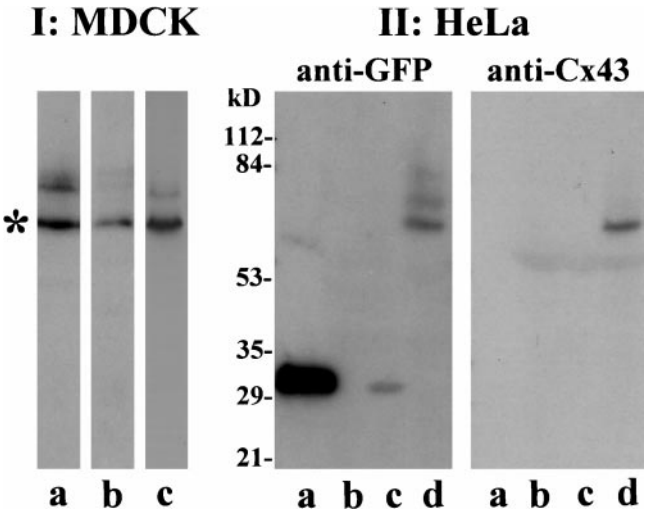

Figure 2. Expression of Cx43-GFP fusion protein in Cx43-deficient MDCK cells and communication-deficient HeLa cells. (I) Lysates of MDCK cells stably expressing Cx43-GFP were resolved by SDS-PAGE, and Western blots were immunolabeled with a polyclonal antibody to GFP (lane a), a polyclonal antibody directed against the amino terminus of Cx43 (lane b), or a monoclonal antibody directed against the carboxyl terminus of Cx43 (lane c). The asterisks denote the position of the major species of the Cx43-GFP fusion protein. (II) Recombinant GFP (lane a), lysates of HeLa cells (lane b), lysates of HeLa cells transiently expressing GFP (lane c), and lysates of HeLa cells transiently expressing Cx43-GFP (lane d) were probed with a polyclonal antibody to GFP and a monoclonal to Cx43 in an immunoblot.

ysis, images were arranged sequentially in a movie sequence on LSM 410 software provided by Zeiss.

RESULTS

Expression of Cx43-GFP in Mammalian Cells

Cx43-deficient MDCK cells were transfected with cDNA encoding Cx43-GFP to examine their ability to biosynthesize full-length Cx43-GFP fusion protein. Western blots of cellular lysates from MDCK cells that express Cx43-GFP immunolabeled with anti-GFP (Figure 2I, lane a), anti-Cx43 polyclonal (Figure 2I, lane b), or anti-Cx43 monoclonal (Figure 2I, lane c) revealed a major protein band at 65 kDa with a minor species at 72 kDa. We also chose to examine whether a communication-incompetent cell line was capable of producing Cx43-GFP. Wild-type HeLa cells were negative for both GFP and Cx43 (Figure 2II, lane b), whereas GFP was resolved at 30 kDa in HeLa cells transfected with cDNA encoding for GFP alone (Figure 2II, lane c). Similar to MDCK cells, the major species of the Cx43-GFP chimera was resolved at 65 kDa in Cx43-GFP–expressing HeLa cells, whereas minor Cx43-GFP species were detected at 72 and 79 kDa (Figure 2II, lane d). Moreover, immunoprecipitation of Cx43-GFP from $^{32}P_i$-labeled cells revealed that the chimera was a phosphoprotein (our unpublished results). Recombinant GFP protein was detected as expected at 30 kDa with an anti-GFP antibody (Figure 2II, lane a).

The Cx43-GFP Chimera Traffics to the Plasma Membrane and Assembles into Gap Junctions

We next chose to examine whether the Cx43-GFP chimera would transport properly to the plasma membrane and form fluorescent puncta at cell–cell interfaces. We used an MDCK cell line that does not express Cx43 as our prototype, because the Cx43-GFP was readily expressed in these cells (Figure 2I). In addition, we transfected cells that were communication deficient (HeLa and N2A) to see whether Cx43-GFP alone was sufficient to form gap junctions, and, finally, we transfected cells that expressed wild-type Cx43 (NRK). In both transiently and stably expressing cell lines, when we observed chimera protein expression by fluorescence, we could observe puncta at cell–cell interfaces (Figures 3-11). Because NRK cells normally express abundant Cx43, transfection with the cDNA for Cx43-GFP would allow us to test whether the presence of the chimera affects native gap junction formation. When Cx43-GFP was expressed in NRK cells, gap junction-like staining was readily observed in fixed cells at interfaces where adjoining cells both expressed Cx43-GFP (Figure 3, B and C, arrows). In addition, gap junction plaques were formed at interfaces between NRK cells expressing GFP-tagged Cx43 and untransfected cells, which likely contribute wild-type Cx43 (Figure 3, C and D, double arrows). Imaging of live NRK cells transfected with cDNA encoding Cx43-GFP also revealed gap junction plaques (Figure 3D, double arrows). In addition, this finding in live cells supports early freeze-fracture results (Zampighi *et al.*, 1988), because it demonstrated that gap junction channel clustering and plaque formation are not artifacts of commonly used fixation or rapid freezing protocols. As a control, imaging of live NRK cells expressing GFP only demonstrated that this protein had no distinct localization pattern and was found in both the cytoplasm and nucleus (Figure 3E). To examine whether the paranuclear distribution of Cx43-GFP observed in NRK cells was due to a Golgi apparatus localization, NRK cells expressing Cx43-GFP (Figure 3F) were labeled with an antibody specific for MG-160, a resident protein of the Golgi apparatus (Figure 3G). MG-160 was found to colocalize with intracellular Cx43-GFP (Figure 3, F and G, arrows).

We also sought to immunologically colocalize Cx43 and GFP in both communication-competent NRK cells and communication-deficient N2A cells (Veenstra *et al.*, 1992) that had been transfected with cDNA encoding Cx43-GFP. Cx43-GFP expressed in NRK cells (Figure 4, A and D) was colocalized with both anti-GFP (Figure 4B) and anti-Cx43 (Figure 4E) antibodies with essentially 100% overlap with the GFP fluorescence (Figure 4, C and

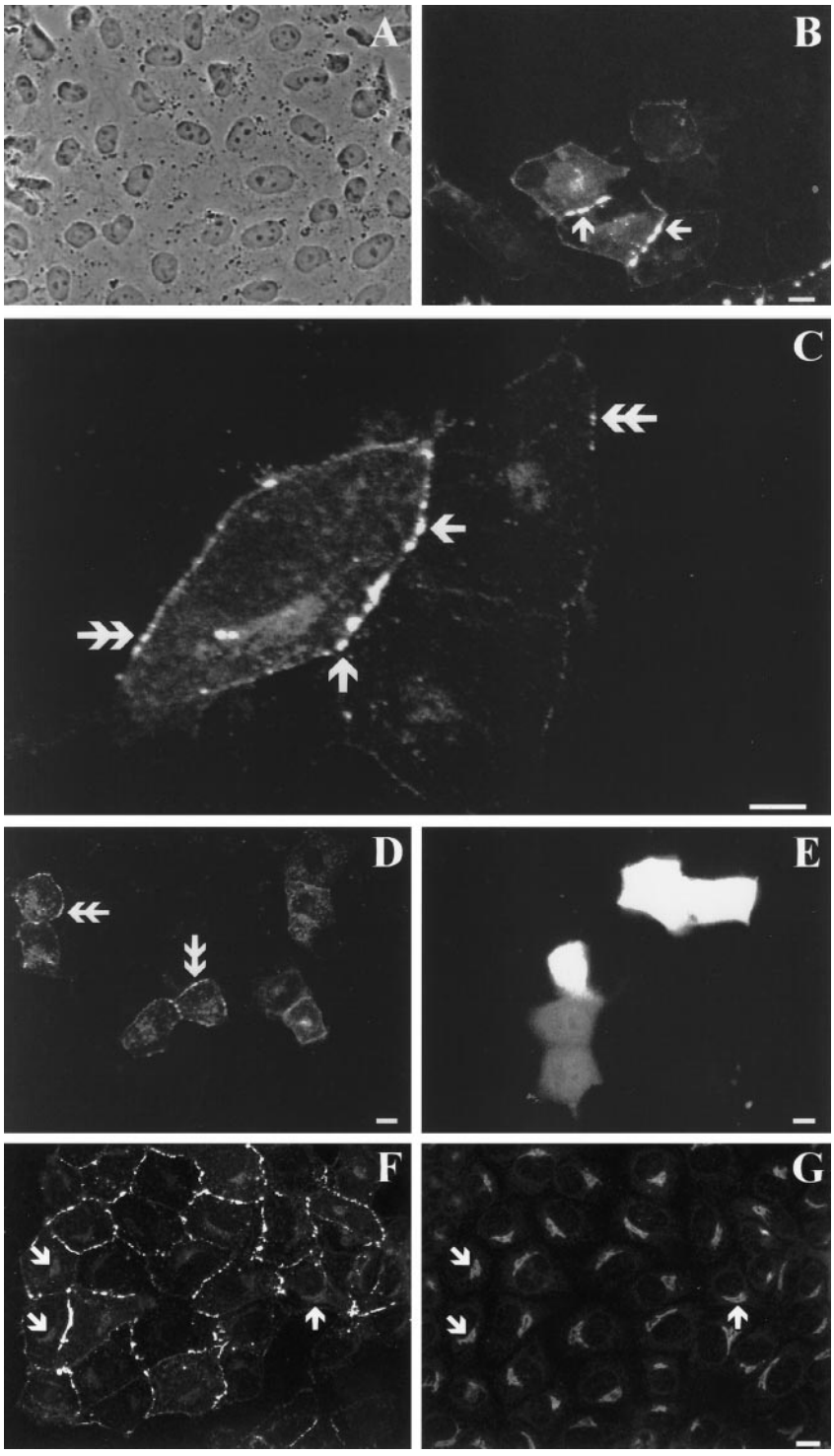

Figure 3. The Cx43-GFP chimera traffics through the Golgi apparatus and assembles into gap junction plaques in NRK cells. NRK cells were transiently transfected with Cx43-GFP, fixed, and imaged on a Zeiss LSM confocal microscope (A, phase view; B, Cx43-GFP fluorescence). (C) Higher-magnification fluorescent image of fixed NRK cells expressing Cx43-GFP. Similar localization patterns of the Cx43-GFP fusion protein were acquired when live cells were imaged (D). GFP transiently expressed in live NRK cells was dispersed throughout the cell (E). Single arrows denote locations where both contacting cells may be contributing GFP-tagged Cx43; double arrows reflect sites where one cell contributes GFP-tagged Cx43 and the adjacent cell likely contributes wild-type Cx43 (C and D). NRK cells stably expressing Cx43-GFP (F) were immunolabeled for the resident Golgi protein MG-160 (G). The arrows denote Cx43-GFP localized within the Golgi apparatus (F and G). Bar, 10 μm.

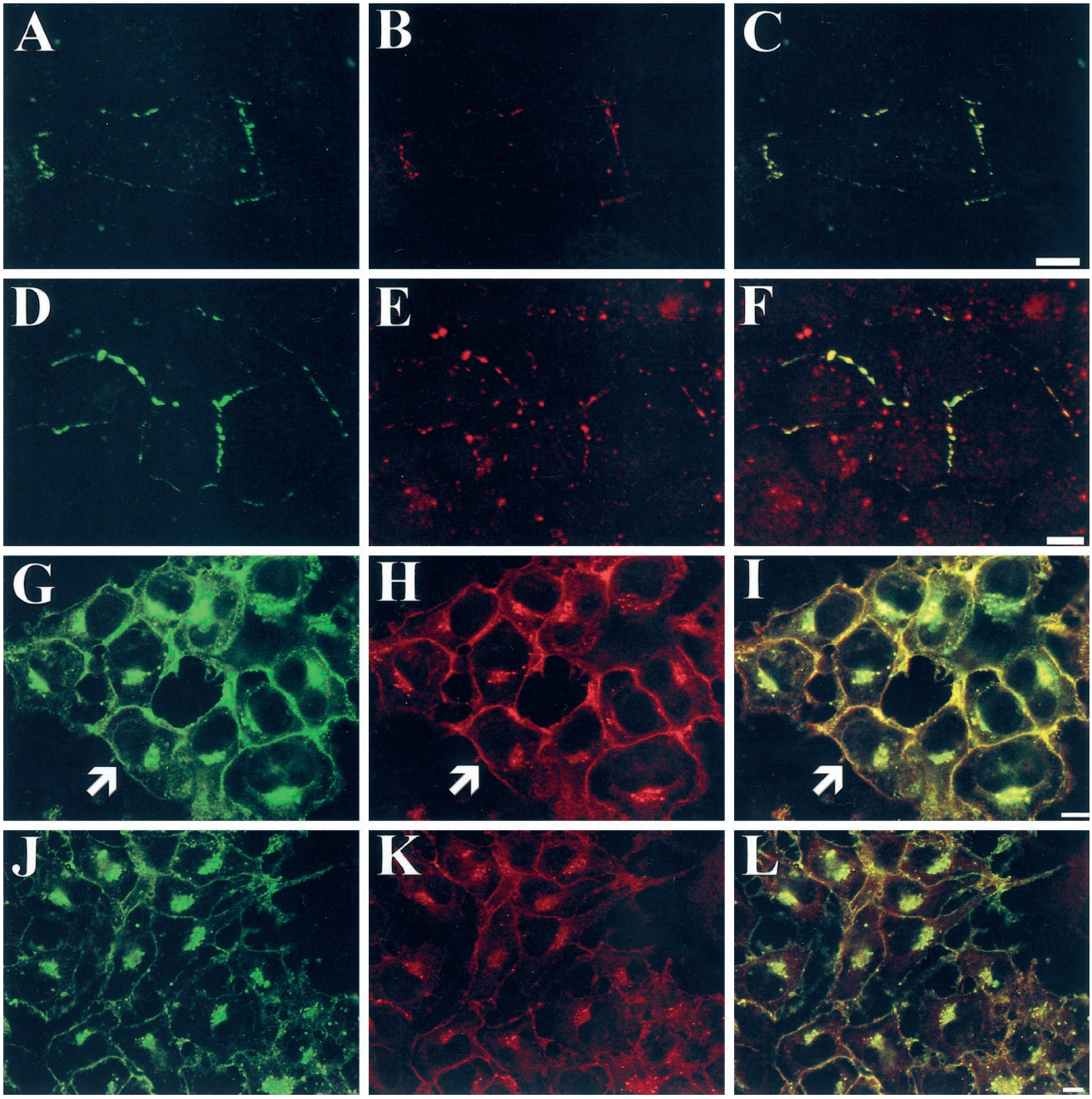

Figure 4. Colocalization of Cx43-GFP fluorescence with immunofluorescently labeled GFP and Cx43 in NRK and N2A cells. NRK cells (A–F) transiently expressing Cx43-GFP (A and D, green) were immunolabeled with anti-GFP (B, red) or anti-Cx43 (E, red) antibodies. In both instances, all of the GFP fluorescence colocalized with the anti-GFP (C, yellow) or anti-Cx43 (F, yellow) antibody-labeled structures. The additional immunostaining observed when NRK cells were labeled with anti-Cx43 antibodies was mostly likely due to the presence of wild-type Cx43 (E and F, red). The fluorescence of Cx43-GFP in N2A cells stably expressing the fusion protein (G and J, green) completely colocalized with the anti-GFP (H, red) and anti-Cx43 (K, red) immunofluorescent labeling patterns (see yellow in overlays; I and L). The arrows denote cell surface localization of Cx43-GFP in N2A cells where the cell does not have an apposed neighbor (G–I). Bar, 10 μm.

F). The additional immunostaining for Cx43 observed in NRK cells was most likely due to the presence of wild-type Cx43 (Figure 4, E and F). GFP fluorescence in N2A cells expressing Cx43-GFP (Figure 4, G and J) colocalized with both anti-GFP (Figure 4H) and anti-Cx43 (Figure 4K) antibody-labeling patterns (Figure 4, I and L), confirming that the fusion protein contains both Cx43 and GFP moieties. Note that N2A cells contained a larger

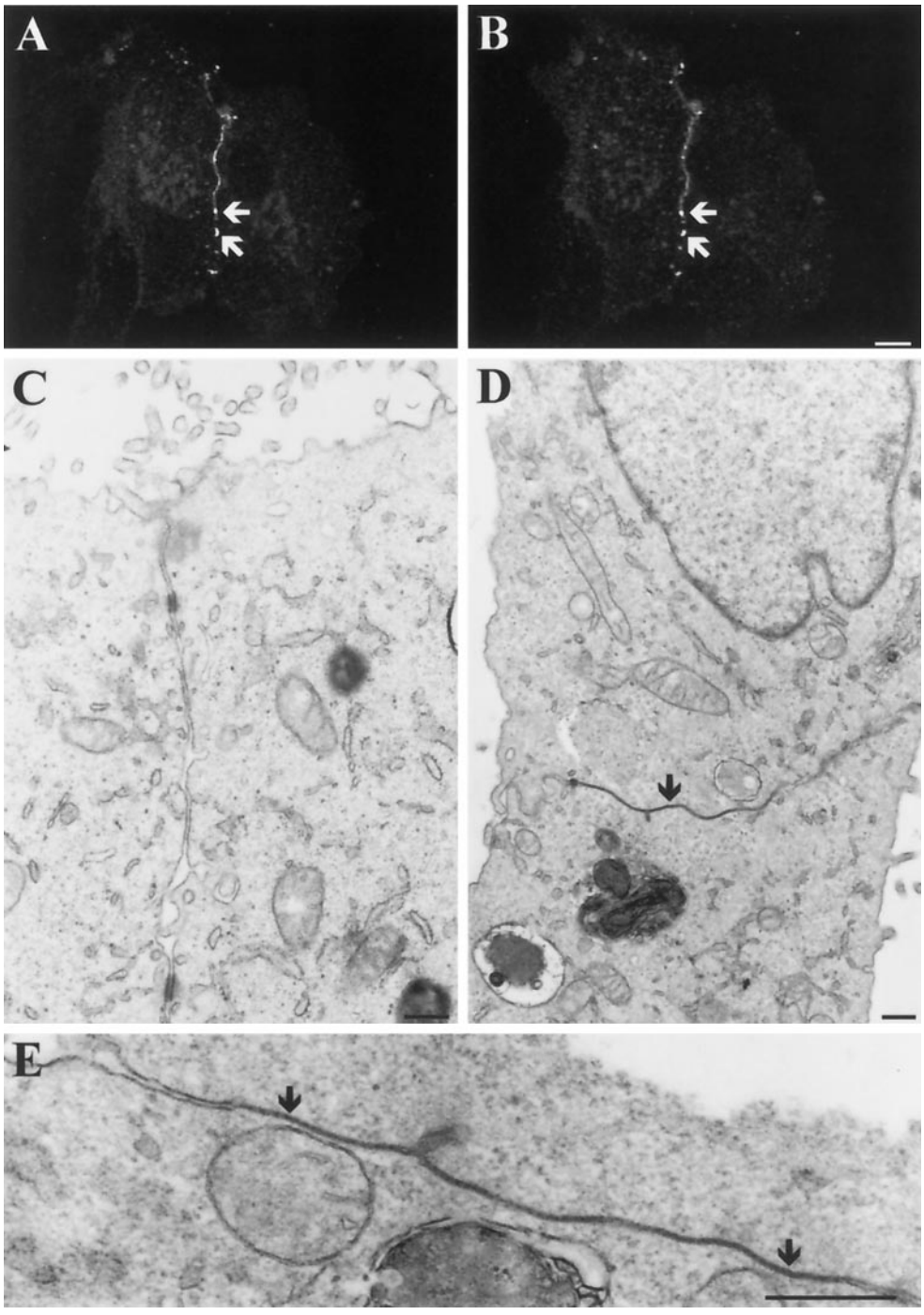

Figure 5. Micrographs of Triton X-100–resistant gap junctions and gap junction plaques in MDCK cells stably expressing Cx43-GFP. Fluorescent images of MDCK cells expressing Cx43-GFP before (A) and after (B) in situ treatment with 1% Triton X-100 for 20 min are shown. Note the presence of fluorescent gap junctions that have properties of being resistant to Triton X-100 (A and B, arrows). MDCK cells (C) or MDCK cells stably expressing Cx43-GFP (D and E) were fixed and prepared for conventional thin-section electron microscopy. Note the presence of large gap junction plaques, which exhibit the classical pentalaminar profile (D and E, arrows). Bar, 10 μm (A and B); 0.5 μm (C–E).

intracellular pool of Cx43-GFP in a paranuclear location reminiscent of the Golgi apparatus (Laird *et al.* 1995) and the Golgi pool of Cx43-GFP observed in NRK cells (Figure 3). Connexin-dependent hemichannel activity has been reported in the plasma membrane of various cell types (Li *et al.*, 1996), but the visualization of Cx43 in

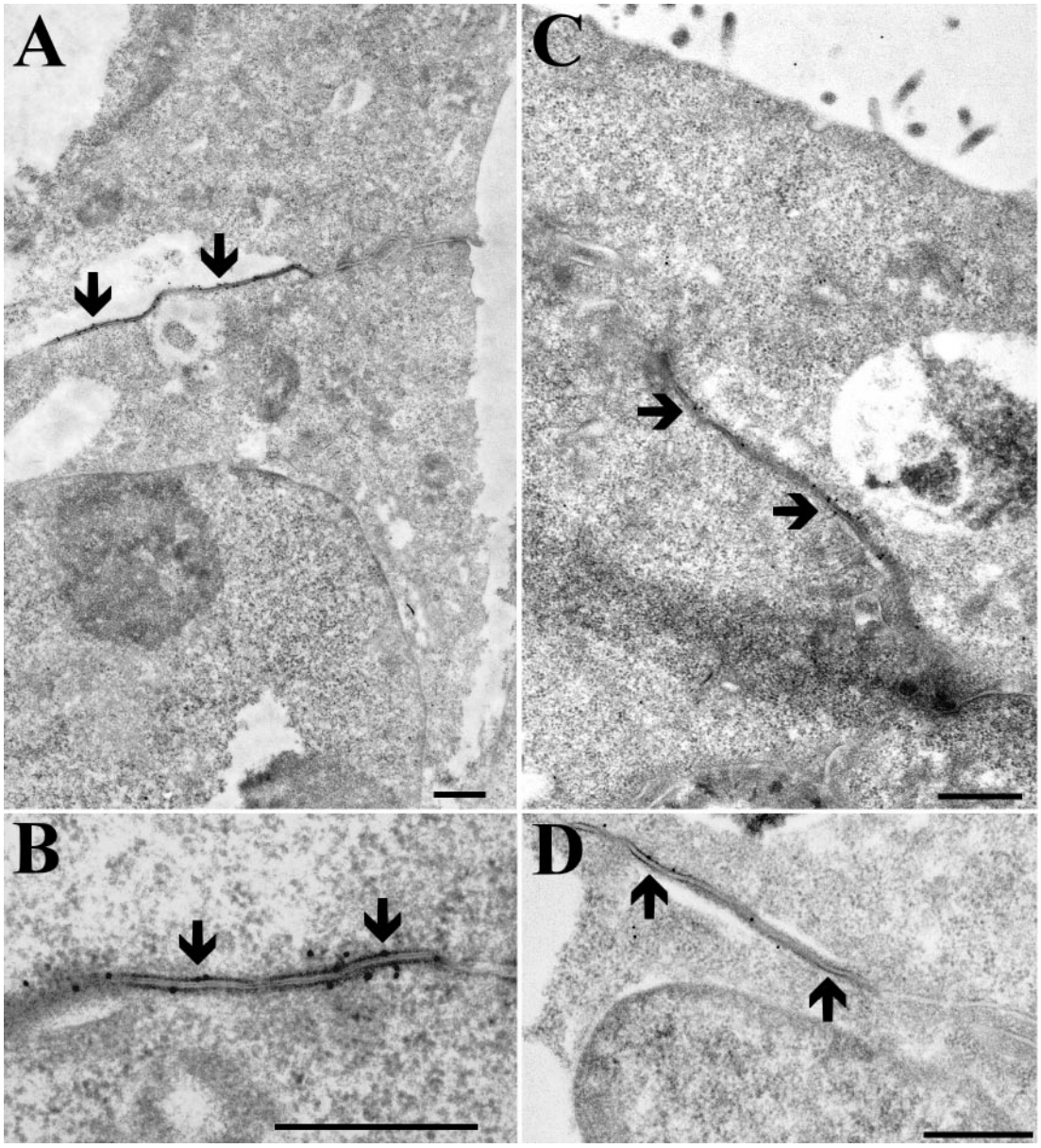

Figure 6. Ultrastructural localization of GFP and Cx43 in MDCK cells stably expressing Cx43-GFP. Thin sections of Lowicryl-embedded, Cx43-GFP-expressing MDCK cells were immunogold labeled for GFP (A and B) or Cx43 (C and D). Note the specific localization of gold particles to the gap junction plaques (arrows). Bar, 0.5 μm.

membranes where cells are not apposed has not been well documented. Localization studies of Cx43-GFP in transfected N2A cells revealed the chimeric protein at the cell surface of both single cells (our unpublished results) and at sites where the transfected N2A cell had no apposed neighbor (Figure 4, arrows).

Cx43-GFP Gap Junction Plaques Are Triton X-100 Resistant and Exhibit Normal Ultrastructure

Gap junctions have the property of being resistant to nonionic detergents (Musil and Goodenough 1991). Therefore, we treated cells with detergent to determine whether the punctate fluorescent staining we observed was also detergent resistant. Live MDCK cells that express Cx43-GFP were imaged (Figure 5A) and then treated with 1% Triton X-100 in situ and reimaged (Figure 5B). Densitometry of the images using NIH-Image (available at http://rsb.info.nih.gov/nih-image) indicated that 54% of the fluorescence intensity was lost in the paranuclear region compared with a reduction of 17% at the cell–cell interface.

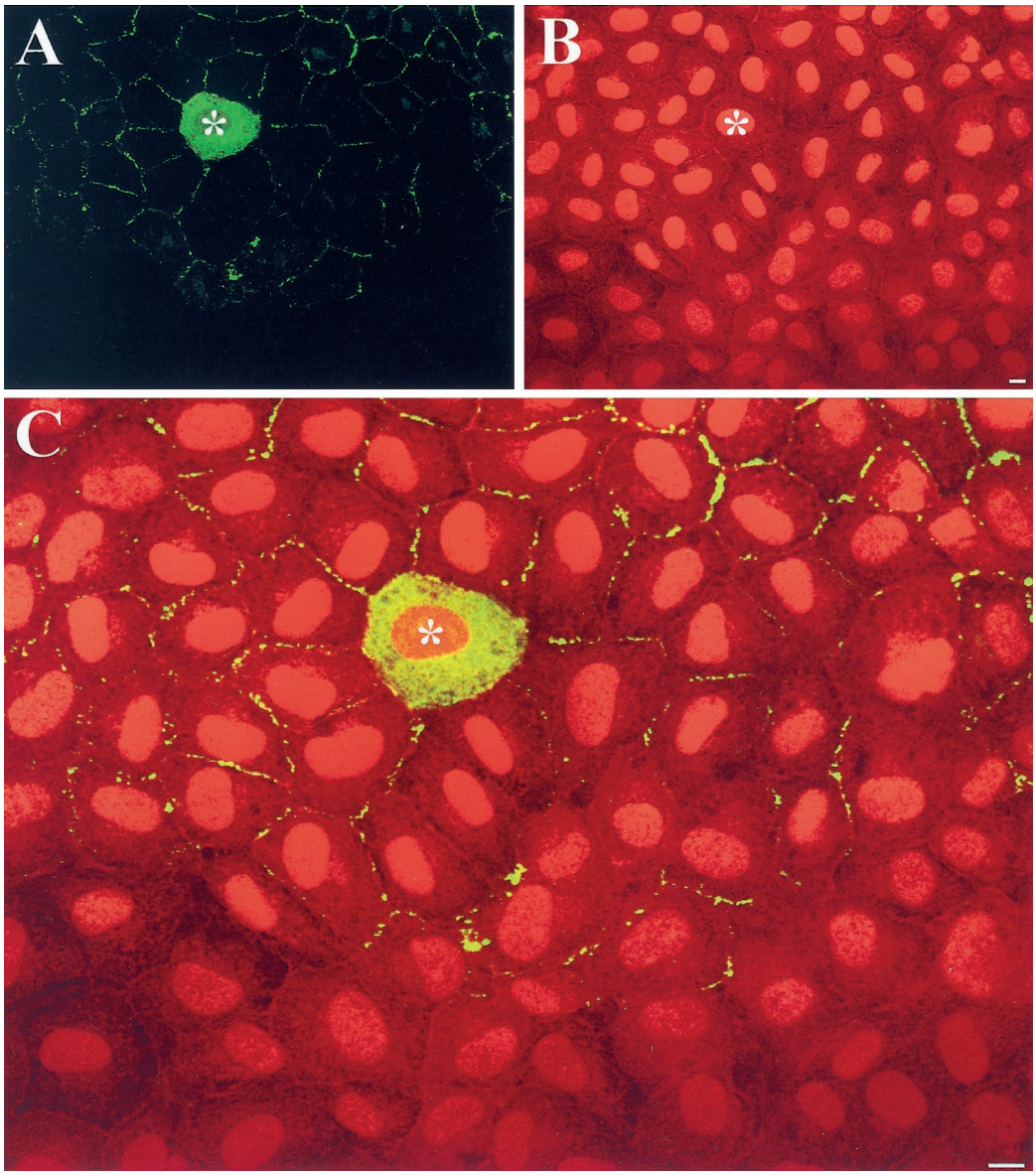

Figure 7. Cx43-GFP does not inhibit gap junction communication in communication-competent NRK cells. NRK cells expressing high levels of Cx43-GFP at the cell surface (A, green) were comicroinjected with Neurobiotin and rat IgG. Cells were fixed, and the microinjected cell and Neurobiotin transfer were monitored by staining the cells with goat anti-rat IgG conjugated to fluorescein (A and C, green cytoplasm of microinjected cell) and streptavidin Texas Red (B and C, red), respectively. Note that neurobiotin transferred extensively from the microinjected cell to cells that expressed high levels of Cx43-GFP (upper part of C) and to cells that did not express detectable levels of the fusion protein (lower part of C). Note that both Cx43-GFP fluorescence and fluorescein-labeled rat IgG show up in the green channel. Bar, 10 μm.

To examine the characteristics of Cx43-GFP at the ultrastructural level, MDCK cells expressing Cx43-GFP were prepared for conventional and immunoelectron microscopy analysis. Although parental MDCK cells were rich in desmosomes and contained many multivesicular bodies, no gap junction plaques were observed by conventional thin-section electron microscopy (Figure 5C), and they were devoid of Cx43 by Western immunoblots (our unpublished results). MDCK cells expressing Cx43-GFP had many large gap junction plaques (Figure 5, D and E). Confirmation that the gap junction plaques observed by thin-section electron microscopy contained the Cx43-GFP fusion protein was provided when thin sections were immunogold labeled for GFP (Figure 6, A and B) or Cx43 (Figure 6, C and D). Gold particles decorating the gap

Table 1. Neurobiotin and Lucifer yellow transfer

Cells	Transfection	Injected molecule	No. of injections	% coupled
NRK	Wild type	Neurobiotin	55	100
NRK + GFP	Transient	Neurobiotin	50	88
NRK + Cx43-GFP	Transient	Neurobiotin	26	100
HeLa	Wild type	Neurobiotin	55	14
HeLa + GFP	Transient	Neurobiotin	47	15
HeLa + Cx43-GFP	Transient	Neurobiotin	74	86
HeLa	Wild type	LY	202	23
HeLa + Cx43-GFP	Stable	LY	217	78
N2A	Wild type	LY	73	4
N2A + Cx43-GFP	Stable	LY	48	93

In functional assays, wild type NRK, HeLa, and N2A cells and cells expressing Cx43-GFP or GFP were microinjected with Neurobiotin or Lucifer yellow (LY) to determine the incidence of gap junction coupling. The number of microinjected cells that resulted in Neurobiotin or LY transfer is expressed as a percent.

junctional plaques are shown in Figure 6 (arrows, all four panels). Together these results strongly suggest that Cx43-GFP was assembled into normal gap junction plaques that exhibit the biochemical property of being Triton X-100 resistant.

Cx43-GFP Does Not Inhibit Gap Junction Communication and Assembles into Functional Gap Junction Channels

To ascertain whether Cx43-GFP can inhibit communication in communication-competent, Cx43-positive NRK cells, one cell in a colony of NRK cells that expressed heterogeneous levels of Cx43-GFP was comicroinjected with Neurobiotin and rat IgG (Figure 7, A and C, green, asterisk). Neurobiotin spread extensively to cells that expressed high levels of Cx43-GFP (Figure 7C, upper region, red) and to NRK cells that appear to have no detectable fusion protein (Figure 7C, lower region, red). The cell that was microinjected was detected by immunolabeling for rat IgG (Figure 7A, green in cytoplasm). Untreated NRK cells, NRK cells expressing GFP, and NRK cells expressing the Cx43-GFP chimera effectively transferred Neurobiotin to greater than 88% of the neighboring cells (Table 1). Transfer was extensive with almost all injections resulting in transfer to fourth tier cells.

To determine whether Cx43-GFP assembles into functional gap junction channels, communication-deficient HeLa cells were stably transfected with cDNA encoding Cx43-GFP. Wild-type HeLa cells (Figure 8A) microinjected with Lucifer yellow (Figure 8B) transferred dye to an average of 0.39 ± 0.13 cells (202 injections; $n = 5$) with 23% of the microinjections exhibiting a very low level of dye coupling (Table 1). Conversely, HeLa cells stably expressing Cx43-GFP (Figure 8C) exhibited a subtle change in morphology and a significant increase in transfer of Lucifer yellow (Figure 8D), with dye spreading to an average of 3.01 ± 0.90 cells ($p < 0.001$; 217 injections) and with 78% of the microinjections exhibiting dye coupling (Table 1). Similar subtle changes in morphology were evident in HeLa cells transfected with wild-type connexin cDNAs (Elfgang *et al.*, 1995). HeLa cells expressing Cx43-GFP also significantly increased their ability to transfer microinjected Neurobiotin (86% of microinjected cells) over the levels observed in untreated HeLa cells (14% of microinjected cells) or HeLa cells that expressed GFP alone (15% of microinjected cells) (Table 1). The low level of apparent dye transfer that occurs occasionally in the absence of Cx43-GFP was often very rapid, most likely due to cytoplasmic bridges that exist between incompletely divided daughter cells. In other cases, cell processes from an adjacent cell may have been injected at the same time as the primary cell. To further examine whether the Cx43-GFP fusion protein was capable of assembling into functional channels in other communication-deficient cells, we also studied N2A cells, because they have been reported to express no known connexins and are unable to form gap junctions (Veenstra *et al.* 1992). N2A cells expressing Cx43-GFP (Figure 8E, arrows) were microinjected with Lucifer yellow (Figure 8F, asterisks), and dye was observed to transfer to multiple neighbors (Figure 8F). In only rare occasions was dye not detected in neighboring cells that expressed Cx43-GFP at cell–cell interfaces, possibly reflecting insufficient time for dye transfer. In quantification studies, wild-type N2A cells essentially showed no Lucifer yellow dye transfer, with only 4% of the injections showing transfer to a single neighbor (Table 1). However, after transfection with Cx43-GFP cDNA, N2A cells exhibited a significant increase in dye coupling, because 93% of the microinjected N2A cells transferred dye (Table 1).

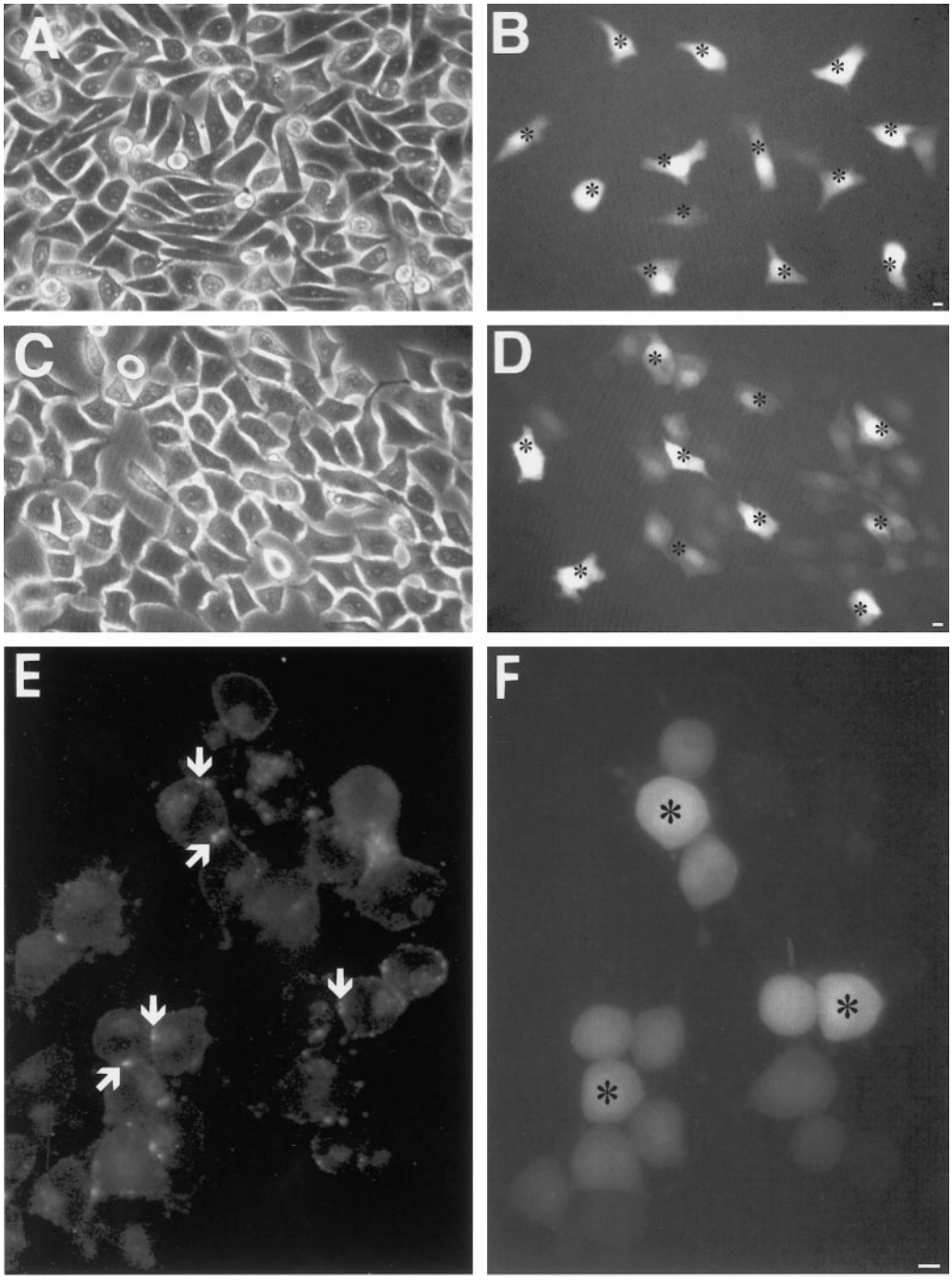

Figure 8. HeLa and N2A cells stably expressing Cx43-GFP are well coupled. HeLa cells microinjected with Lucifer yellow rarely exhibited dye transfer to neighboring cells, as shown in phase (A) and fluorescent (B) views. However, when Lucifer yellow was microinjected into HeLa cells stably expressing Cx43-GFP, dye spread to a number of neighboring cells (C and D). Likewise, when apposed N2A cells expressing Cx43-GFP (E, arrows) were microinjected with Lucifer yellow, dye transferred to several neighboring cells (F). Asterisks mark the injected cells. Bar, 10 μm.

Real-Time Cell Surface Clustering of Cx43-GFP Gap Junctions

To examine the fate of Cx43-GFP present at the cell surface and in apparent gap junction structures, live MDCK cells were imaged for 37.3 min (Figure 9). Although, the majority of assembled gap junction plaques moved short distances (0.05 μm) back and forth, they remained relatively stationary during the time series of

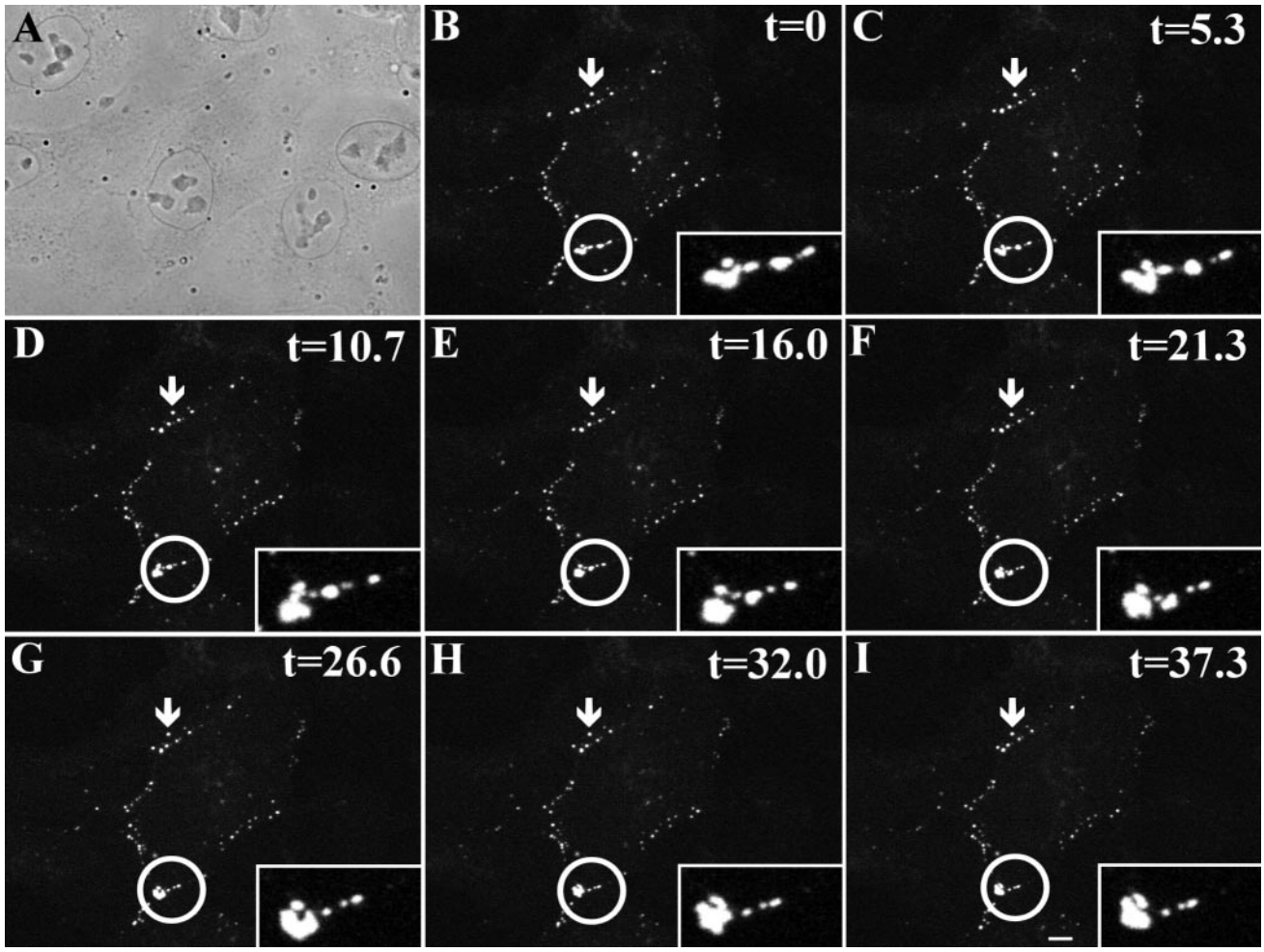

Figure 9. Time series showing the dynamics of gap junction plaques within the plasma membrane of live MDCK cells. MDCK cells stably expressing Cx43-GFP were imaged on a Zeiss inverted confocal microscope over 37.3 min as described in MATERIALS AND METHODS. The arrows denote a gap junction plaque that remains relatively stationary throughout the time course of the experiment (B–I). Enclosed within the circle are several fluorescent gap junctions that coalesced within the plasma membrane. Insets represent an area at higher magnification where gap junctions undergo clustering. t = min; bar, 10 μm. (Online version available at www.molbiolcell.org.)

images (Figure 9, arrow). This observation also demonstrated that the cells were not moving during the time course of the experiment. However, several fluorescent gap junction plaques moved within the plasma membrane and coalesced during the 37.3-min time series (Figure 9, circle, insets). An interesting feature of intracellular Cx43-GFP that cannot be effectively demonstrated in static images (Figure 9) but is apparent when the data are presented as a QuickTime movie sequence is that intracellular transport intermediates migrate rapidly, and somewhat randomly, within the cell (online version for Figure 9 available at www.molbiolcell.org).

Cx43-GFP Trafficking Involves Two Populations of Transport Intermediates

To further examine the size and track the mobility of Cx43 transport intermediates, additional time-lapse imaging was performed on MDCK cells that expressed Cx43-GFP. The pool of Cx43-GFP transport intermediates that exists in MDCK cells was found to be both heterogeneous and differentially mobile (Figure 10). Although the resolution of the fluorescence microscope is not sufficient to determine whether these transport intermediates have strict vesicular characteristics, they possess properties consistent with other GFP chimeras of exported proteins and peptides (Kaether and Gerdes 1995; Burke *et al.*, 1997; Kaether *et al.*, 1997; Wacker *et al.* 1997). Clearly there were at least two subfamilies of Cx43-GFP transport intermediates observed within MDCK cells. Given that there is a resolution limit with fluorescent microscopy of 0.2 μm, we chose to subcategorize the transport intermediates into small $<$0.5-μm (Figure 10F, arrows) and large 0.5- to 1.5-μm categories (Figure 10F, double

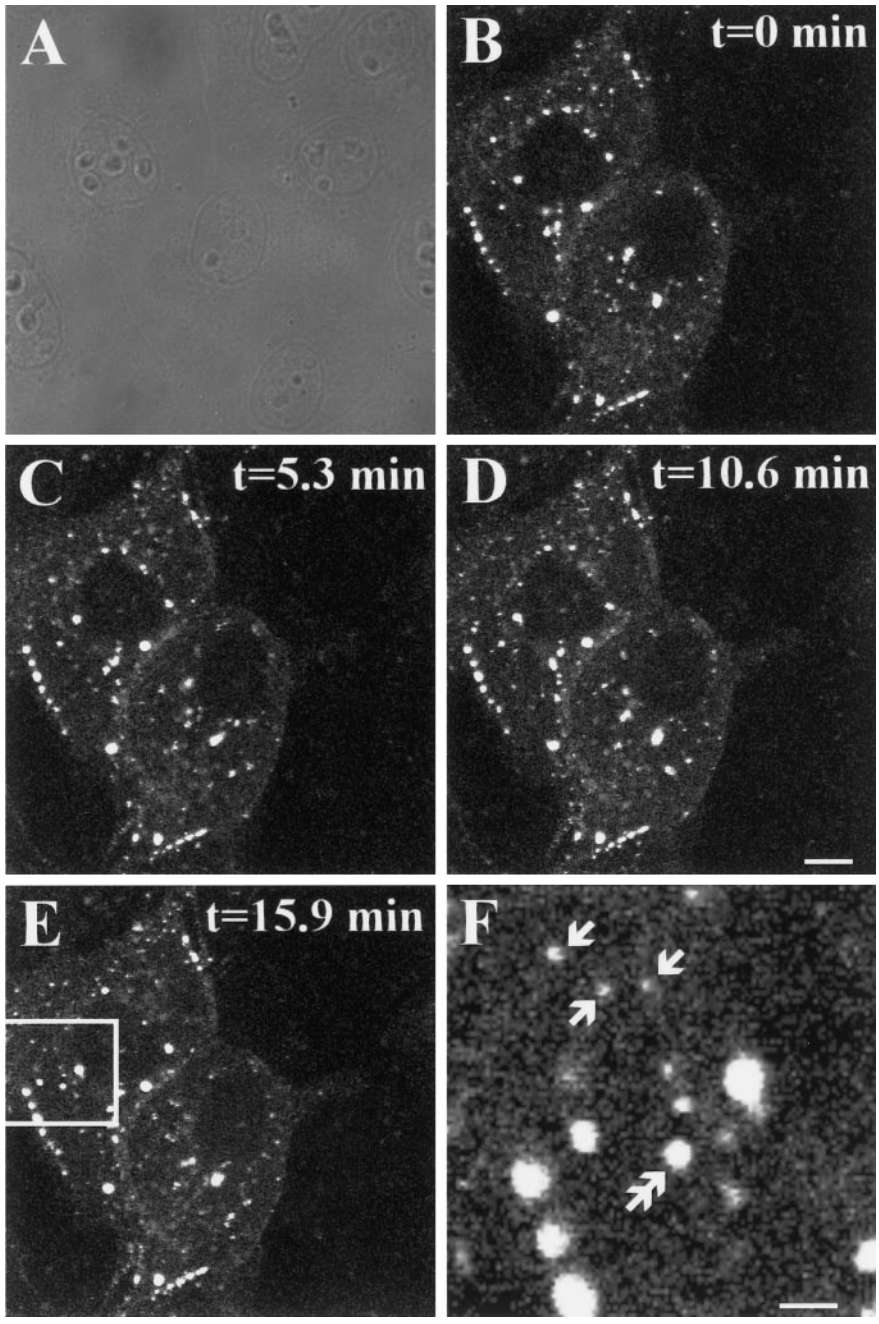

Figure 10. Two populations of transport intermediates are involved in trafficking Cx43-GFP. Live MDCK cells (A) stably expressing Cx43-GFP were time lapsed imaged over 15.9 min (B–E). A region of E is shown at higher magnification in F to illustrate the two populations of transport intermediates (arrows indicate <0.5-μm small transport intermediates; double arrows indicate 0.5- to 1.5-μm large transport intermediates). t = min. Bars: D, 10 μm; F, 2 μm. (Online version available at www.molbiolcell.org.)

arrows). The smaller transport intermediates were typically more numerous, but time series imaging revealed that both populations of transport intermediates were highly mobile (online version for Figure 10 available at www.molbiolcell.org). On occasion, we have observed small transport intermediates apparently fusing with the plasma membrane, suggesting that they represent part of the secretory pathway (our unpublished results).

Budding and Internalization of Cx43-GFP Gap Junctions in Real Time

To examine the possibility that some of the large transport intermediates originated from the internalization of gap junctions or pieces of gap junctions, we followed the fate of cell surface gap junctions in live MDCK cells that express Cx43-GFP. In the course of 96 s, a piece of a gap junction appeared to bud and separate from a row of existing gap junction plaques (Figure 11, C and D, arrows, insets). We

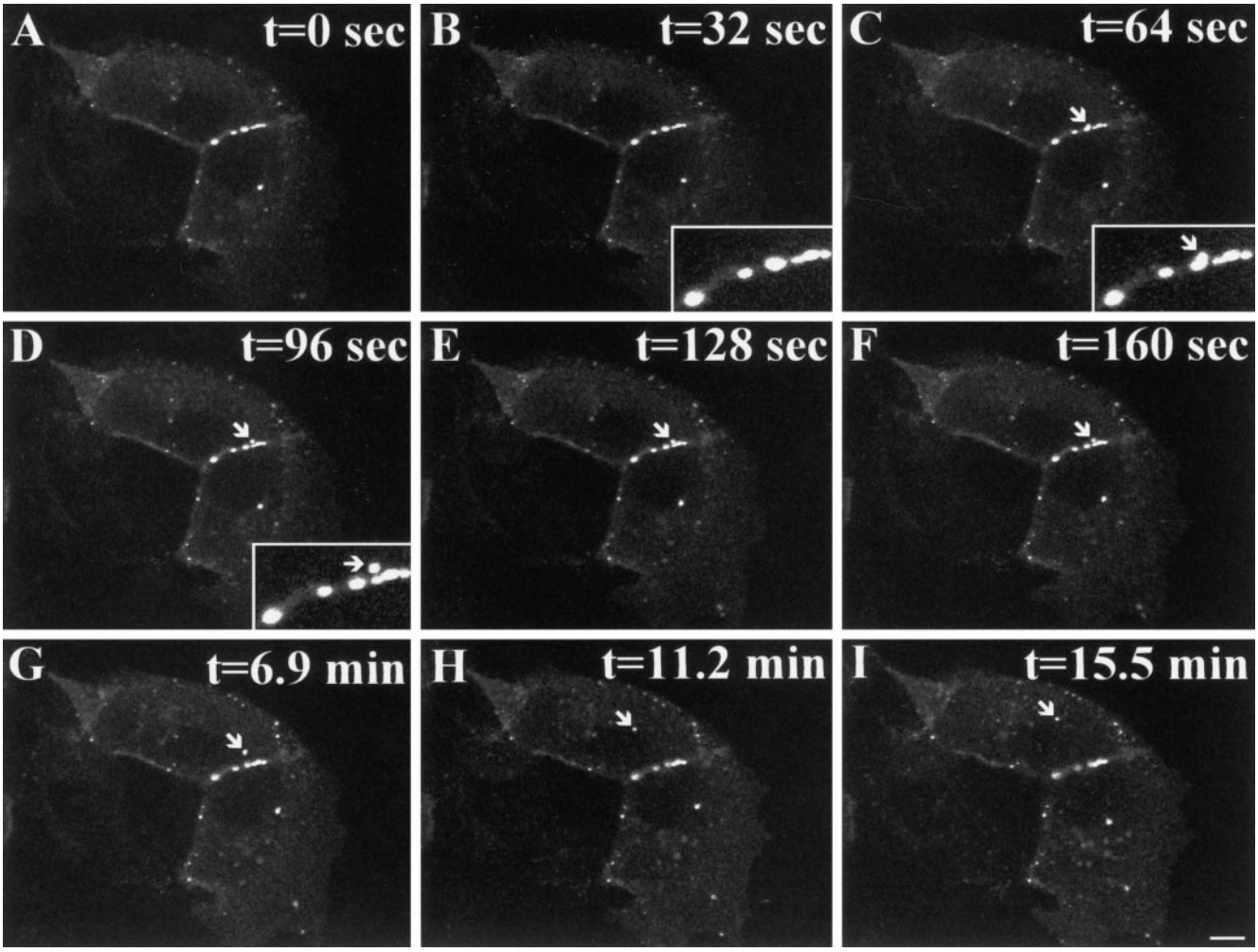

Figure 11. Internalization of a gap junction in real time. Live MDCK cells expressing Cx43-GFP were time-lapse imaged over 15.5 min. The budding and internalization of a gap junction fragment are demonstrated in consecutive 32-s images (A–F). Insets represent the area of gap junction budding and internalization at higher magnification (B–D). G–I follow the fate of the internalized gap junction (arrow) over a total period of 15.5 min. Bar, 10 μm. (Online version available at www.molbiolcell.org.)

believe gap junctions or gap junction fragments indeed bud from the plasma membrane, because these events were frequent, and it is possible to see a reduction in the size of the cell surface gap junction from which the bud originated (Figure 11, compare B and D insets). Time-lapse imaging revealed that within minutes this internalized gap junction migrated to a perinuclear position within the cytoplasm (Figure 11, E–I, arrow; online version for Figure 11 available at www.molbiolcell.org). This process of gap junction internalization may account for a significant population of the large Cx43-GFP transport intermediates that are seen in MDCK cells.

DISCUSSION

To examine the mechanisms of how Cx43 is transported to the plasma membrane and assembled in mammalian cells, we engineered and expressed a Cx43-GFP chimera that exhibits properties and characteristics of wild-type Cx43. The fusion protein electrophoresed as a major protein band at 65 kDa, which appears to be fully intact, because it was detected using multiple antibodies to the N- and C-terminal portions of Cx43 and to GFP. Moreover, Cx43-GFP was found to be a phosphoprotein consistent with wild-type Cx43 (Crow *et al.*, 1990; Laird and Revel 1990; Laird *et al.*, 1991; Musil *et al.*, 1990; Musil and Goodenough, 1991). We have not ruled out the possibility that a portion of Cx43-GFP may be ubiquitinated, because wild-type Cx43 has been shown to be a suitable substrate for ubiquitination (Laing and Beyer 1995). When this fusion protein was expressed in a variety of communication-competent and -incompe-

tent mammalian cells, it was efficiently transported to the cell surface and assembled into gap junction plaques. Comparative studies of fixed and live cells, which expressed Cx43-GFP, revealed that clustering of gap junction channels was not induced by fixation procedures but rather was an inherent feature of gap junctions in living cells. Ultrastructural analysis revealed that the Cx43-GFP chimera was assembled into large gap junction plaques that exhibit the classic pentalaminar, gap junctional profile. Previously, it has been demonstrated that gap junction plaques assembled from wild-type Cx43 exhibit a resistance to Triton X-100 solubility (Musil and Goodenough 1991). Similarly, gap junction plaques assembled from Cx43-GFP also exhibit a resistance to Triton X-100 in situ. Consequently, based on biochemical and morphological parameters, gap junctions assembled from Cx43-GFP exhibit the same characteristics as gap junctions assembled from wild-type Cx43.

We investigated the possibility that Cx43-GFP might inhibit communication in communication-competent cells because expression of a Cx43-β-galactosidase fusion protein inhibited gap junctional communication in NIH3T3 cells (Sullivan and Lo 1995). However, functional studies in NRK cells that expressed low to high levels of Cx43-GFP showed extensive Neurobiotin transfer, eliminating the possibility that the fusion protein was capable of inhibiting communication in communication-competent NRK cells at these levels of protein expression. More importantly, when Cx43-GFP was expressed in communication-deficient HeLa or N2A cells, functional channels capable of passing both Lucifer yellow and/or Neurobiotin were assembled. These results were consistent with the findings of Martin *et al.* (1998), in which Cx43-aequorin fusion protein was found to assemble into functional gap junction channels in communication-deficient HeLa cells. Whether Cx43-GFP is being assembled into homomeric channels or recruiting undefined connexins from the communication-deficient HeLa or N2A cells remains unclear. Given that both of these cell types have no apparent expression of endogenous connexins and are communication deficient, we propose that homomeric channels composed of Cx43-GFP are functional. This conclusion is further supported by recent electrophysiological recordings on N2A cells that express punctate Cx43-GFP at cell–cell interfaces (e.g., Figure 8E). Electrical coupling in these cells was only observed when plaques were visible via intrinsic Cx43-GFP fluorescence, and the single-channel conductance observed was very similar to wild-type (~100 pS) Cx43 channels (Verselis, personal communication).

The generation of a Cx43-GFP chimera that exhibits wild-type Cx43 characteristics allowed us to address the mechanisms of connexin trafficking and gap junction assembly in living cells. Consistent with previous biochemical and functional studies that showed that Cx43 gap junction hemichannels exist on the surface of mammalian cells (Beyer and Steinberg 1991; Li *et al.* 1996), we were able to visualize constitutive levels of nonjunctional Cx43-GFP on the surface of N2A transfectants. This finding suggests that there is no requirement for a cell–cell contact signal for Cx43-GFP to traffic to the cell surface. This is particularly interesting because we and others have shown that a calcium-dependent cell–cell adhesion event is necessary for gap junction plaque channel formation (Musil *et al.* 1990; Jongen *et al.*, 1991; Meyer *et al.*, 1992). It may be the case that some clones of N2A cells, which express relatively large amounts of Cx43-GFP, are not efficient at forming adherens and gap junctions. This results in a cell surface accumulation of nonjunctional Cx43-GFP, as may be the case when some wild-type connexins are expressed in N2A cells (Rup *et al.*, 1993). However, because we can also observe low levels of nonjunctional Cx43-GFP in other mammalian cells, we suggest that the sensitivity of red-shifted GFP when fused to Cx43 allows for an apparent visualization of hemichannel intermediates in channel formation. Together, these results would suggest that downstream signaling via cadherins is not necessary for recruitment of connexins or Cx43-GFP to the cell surface but is probably necessary for junctional channel formation.

It has been known for some time that connexins are dynamic molecules with half-lives of 1–5 h (Fallon and Goodenough 1981; Traub *et al.*, 1987; Laird *et al.* 1991). The results from connexin pulse–chase studies suggest that gap junctions are constantly being formed and removed from the cell surface. Because the Cx43-GFP fusion protein exhibited characteristics of wild-type Cx43, it was possible to examine the life cycle of a connexin in living cells including the transport mechanisms involved in delivering connexins to the plasma membrane, the mobility of gap junctions within the plasma membrane, and the removal of gap junctions from the cell surface. Time-lapse imaging of Cx43-GFP revealed that gap junction plaques within the plasma membrane exhibit a range of mobility. It is possible to speculate that the relative immobility of the majority of gap junction plaques is due to a direct or indirect attachment to the cytoskeletal network. Although microfilaments have been reported to be necessary for Cx43 channel clustering (Wang and Rose 1995), it remains unclear as to role of cytoskeletal elements in plaque formation or maintenance. The resistance of many Cx43-GFP gap junctions to Triton X-100 in situ further suggests that many gap junctions are likely to be relatively immobile within the plasma membrane. In some areas of the plasma membrane, time-lapse imaging revealed that gap junctions are mobile and coalesce to form large fluorescent clusters. It is unlikely that membrane ruffling, which character-

istically occurs at free cell edges, can account for the coalescence and changes in the shape of Cx43-GFP fluorescent signals within the plasma membrane as this dynamic movement of gap junctions occurs at sites of cell–cell contact. Although our ultrastructural analysis of MDCK cells expressing Cx43-GFP revealed large gap junction plaques, it is not possible to determine whether plaques are fusing within the plasma membrane. Moreover, whether laterally mobile gap junction plaques represent newly formed gap junctions or gap junctions that are soon to be internalized and degraded remains to be investigated.

A prominent feature of our time-lapsed movies of MDCK cells that express Cx43-GFP is the persistence of intracellular transport intermediates. Based on the apparent size of the fluorescence emanating from the GFP moiety and the limits of fluorescent microscopy, we have subcategorized these structures as small (<0.5 μm) and large (0.5–1.5 μm). An interesting feature of both populations of Cx43-GFP transport intermediates is that they exhibit rapid, intermittent, and somewhat random movement often migrating distances of 5–10 μm. The rapid movement of the Cx43-GFP transport intermediates may reflect a microtubule-dependent mechanism, which has previously been proposed for the chromogranin B-GFP–positive vesicles (Wacker *et al.* 1997). In preliminary studies, we have demonstrated that the total distance of displacement was reduced in both small and large transport intermediates by ~50% when cells are treated with nocodazole (our unpublished results), suggesting that microtubules play a role in Cx43-GFP trafficking. The fact that the smaller Cx43-GFP transport intermediates represent a size reminiscent of untagged or GFP-tagged secretory vesicles (Oberhauser and Fernandez 1995; Chen *et al.*, 1996; Chen *et al.*, 1997; Burke *et al.* 1997; Wacker *et al.* 1997) suggests that these structures may represent transport of Cx43-GFP to the cell surface. Although further investigation is necessary, in some movie sequences these small transport intermediates that exhibit short periods of directed movement have occasionally been observed to associate with the plasma membrane.

Experimentally, we were able to determine that at least a portion of the larger transport intermediates were generated from the rapid budding and internalization of gap junction fragments. Time-lapse imaging revealed that only one cell of an adjoining pair of cells internalized the entire gap junction fragment, and no splitting of gap junctions has been observed to date. These internalized gap junctions may be similar or identical to the annular gap junctions that have been seen in electron micrographs (Larsen and Hai 1978; Severs *et al.*, 1989; Naus *et al.*, 1993; Murray *et al.*, 1997). In some cases, these internalized gap junctions could be followed as they migrated away from the cell surface, whereas in other cases they disappeared quickly, possibly because of degradation. At present it is not possible to determine whether all of the large intracellular transport intermediates that we observe in living cells originate from the internalization of a gap junction, but it appears that this represents at least one pathway for gap junction removal. An alternative pathway that may exist for removal of gap junctions could be dispersal or degradation of the plaque in situ. In N2A cells, we have observed punctate fluorescence that decreases rapidly in intensity in a manner that is not indicative of photobleaching. To date, we have not been able to reliably follow the fate of Cx43-GFP in living cells for more than 40 min because of photobleaching, stage shifting, and optical drift. Once these technical limitations have been overcome, we plan to examine the assembly and fate of individual gap junctions for several hours and correlate connexin half-lives with gap junction plaque turnover. Nevertheless, in our live cell studies we have obtained convincing evidence of gap junction internalization (Figure 11), which we believe represents a part of the turnover cycle. Consequently, although one might consider many Cx43-GFP gap junction plaques to be static, we expect that they are dynamic, as would be predicted from the turnover kinetics of wild-type Cx43.

In summary, we have engineered and characterized a novel Cx43-GFP fusion protein, which maintains many characteristics of wild-type Cx43, including its ability to oligomerize and assemble into functional gap junction channels. The tracking of Cx43-GFP in living cells has allowed us to identify two populations of highly mobile transport intermediates that are involved in trafficking Cx43-GFP during dynamic gap junction renewal. Time-lapse imaging also revealed that the larger transport intermediates are generated from the internalization of gap junctions or fragments of gap junctions. Analysis of living cells also revealed that many gap junctions are relatively immobile, whereas others cluster at the cell surface, suggesting possible direct or indirect transient linkages to cytoskeletal elements. This fusion protein, when expressed and examined in living cells, will continue to allow us to elucidate the mechanism(s) and regulation of gap junction assembly and removal from the cell surface in steady-state cells and during cell division.

ACKNOWLEDGMENTS

We thank Drs. J.J.M. Bergeron, P. Walton, and Q. Shao for helpful insights and comments on this study. We also thank Lana Tan and Jon Gordon for assistance in generating and customizing the movies. This research was supported by Medical Research Council of Canada operating grant MT-12241 (to D.W.L.) and National Institutes of Health research grant GM-55632 (to P.D.L.). M.D. was supported by a Medical Research Council of Canada grant (to Dr. Bergeron).

REFERENCES

Barak, L.S., Ferguson, S.S., Zhang, J., Martenson, C., Meyer, T., and Caron, M.G. (1997). Internal trafficking and surface mobility of a functionally intact beta2-adrenergic receptor-green fluorescent protein conjugate. Mol. Pharmacol. *51*, 177–184.

Bergoffen, J., Scherer, S.S., Wang, S., Scott, M.O., Bone, L.J., Paul, D.L., Chen, K., Lensch, M.W., Chance, P.F., and Fischbeck, K.H. (1993). Connexin mutations in X-linked Charcot-Marie-Tooth disease. Science. *262*, 2039–2042.

Beyer, E.C., and Steinberg, T.H. (1991). Evidence that the gap junction protein connexin-43 is the ATP-induced pore of mouse macrophages. J. Biol. Chem. *266*, 7971–7974.

Bruzzone, R., White, T.W., and Paul, D.L. (1996). Connections with connexins: the molecular basis of direct intercellular signaling. Eur. J. Biochem. *238*, 1–27.

Burke, N.V., Han, W., Li, D., Takimoto, K., Watkins, S.C., and Levitan, E.S. (1997). Neuronal peptide release is limited by secretory granule mobility. Neuron *19*, 1095–1102.

Chalfie, M., Tu, Y., Euskirchen, G., Ward, W.W., and Prasher, D.C. (1994). Green fluorescent protein as a marker for gene expression. Science *263*, 802–805.

Chen, D., Zhao, C.M., Andersson, K., Sundler, F., and Hakanson, R. (1996). Ultrastructure of enterochromaffin-like cells in rat stomach: effects of alpha-fluoromethylhistidine-evoked histamine depletion and hypergastrinemia. Cell Tissue Res. *283*, 469–478.

Chen, Y.G., Siddhanta, A., Austin, C.D., Hammond, S.M., Sung, T.C., Frohman, M.A., Morris, A.J., and Shields, D. (1997). Phospholipase D stimulates release of nascent secretory vesicles from the trans-Golgi network. J. Cell Biol. *138*, 495–504.

Crow, D.S., Beyer, E.C., Paul, D.L., Kobe, S.S., and Lau, A.F. (1990). Phosphorylation of connexin43 gap junction protein in uninfected and Rous sarcoma virus-transformed mammalian fibroblasts. Mol. Cell. Biol. *10*, 1754–1763.

De Bruijn, W.C. (1973). Glycogen, its chemistry and morphologic appearance in the electron microscope: a modified OsO4 fixative which selectively contrasts glycogen. J. Ultrastruct. Res. *42*, 29–50.

Dobson, S.P., Livingstone, C., Gould, G.W., and Tavare, J.M. (1996). Dynamics of insulin-stimulated translocation of GLUT4 in single living cells visualized using green fluorescent protein. FEBS Lett. *393*, 179–184.

Elfgang, C., Eckert, R., Lichtenberg-Frate, H., Butterweck, A., Traub, O., Klein, R.A., Hulser, D.F., and Willecke, K. (1995). Specific permeability and selective formation of gap junction channels in connexin-transfected HeLa cells. J. Cell Biol. *129*, 805–817.

Essner, J.J., Laing, J.G., Beyer, E.C., Johnson, R.G., and Hackett, P.B., Jr. (1996). Expression of zebrafish connexin43.4 in the notochord and tail bud of wild-type and mutant no tail embryos. Dev. Biol. *177*, 449–462.

Fallon, R.F., and Goodenough, D.A. (1981). Five-hour half-life of mouse liver gap-junction protein. J. Cell Biol. *90*, 521–526.

Flagg-Newton, J., and Loewenstein, W.R. (1979). Experimental depression of junctional membrane permeability in mammalian cell culture. A study with tracer molecules in the 300 to 800 Dalton range. J. Membr. Biol. *50*, 65–100.

Gonatas, J.O., Mezitis, S.G.E., Stieber, A., Fleischer, B., and Gonatas, N.K. (1989). MG-160: a novel sialoglycoprotein of the medial cisternae of the Golgi apparatus. J. Biol. Chem. *264*, 646–653.

Goodenough, D.A., Goliger, J.A., and Paul, D.L. (1996). Connexins, connexons, and intercellular communication. Ann. Rev. Biochem. *65*, 475–502.

Hanakam, F., Albrecht, R., Eckerskorn, C., Matzner, M., and Gerisch, G. (1996). Myristoylated and nonmyristoylated forms of the pH sensor protein hisactophilin II: intracellular shuttling to plasma membrane and nucleus monitored in real time by a fusion with green fluorescent protein. EMBO J. *15*, 2935–2943.

Jongen, W.M., Fitzgerald, D.J., Asamoto, M., Piccoli, C., Slaga, T.J., Gros, D., Takeichi, M., and Yamasaki, H. (1991). Regulation of connexin 43-mediated gap junctional intercellular communication by Ca2+ in mouse epidermal cells is controlled by E-cadherin. J. Cell Biol. *114*, 545–555.

Kaether, C., and Gerdes, H.H. (1995). Visualization of protein transport along the secretory pathway using green fluorescent protein. FEBS Lett. *369*, 267–271.

Kaether, C., Salm, T., Glombik, M., Almers, W., and Gerdes, H.H. (1997). Targeting of green fluorescent protein to neuroendocrine secretory granules: a new tool for real time studies of regulated protein secretion. Eur. J. Cell Biol. *74*, 133–142.

Kelsell, D.P., Dunlop, J., Stevens, H.P., Lench, N.J., Liang, J.N., Parry, G., Mueller, R.F., and Leigh, I.M. (1997). Connexin 26 mutations in hereditary nonsyndromic sensorineural deafness. Nature *387*, 80–83.

Komatsu, H., Mori, I., Rhee, J.S., Akaike, N., and Ohshima, Y. (1996). Mutations in a cyclic nucleotide-gated channel lead to abnormal thermosensation and chemosensation in *C. elegans*. Neuron *17*, 707–718.

Laing, J.G., and Beyer, E.C. (1995). The gap junction protein connexin43 is degraded via the ubiquitin proteasome pathway. J. Biol. Chem. *270*, 26399–26403.

Laird, D.W. (1996). The life cycle of a connexin: gap junction formation, removal, and degradation. J. Bioenerg. Biomembr. *28*, 311–318.

Laird, D.W., Castillo, M., and Kasprzak, L. (1995). Gap junction turnover, intracellular trafficking, and phosphorylation of connexin43 in brefeldin A-treated rat mammary tumor cells. J. Cell Biol. *131*, 1193–203.

Laird, D.W., Puranam, K.L., and Revel, J.P. (1991). Turnover and phosphorylation dynamics of connexin43 gap junction protein in cultured cardiac myocytes. Biochem. J. *273*, 67–72.

Laird, D.W., and Revel, J.P. (1990). Biochemical and immunochemical analysis of the arrangement of connexin43 in rat heart gap junction membranes. J. Cell Sci. *97*, 109–117.

Larsen, W.J., and Hai, N. (1978). Origin and fate of cytoplasmic gap junctional vesicles in rabbit granulosa cells. Tissue Cell *10*, 585–598.

Li, H., Liu, T.F., Lazrak, A., Peracchia, C., Goldberg, G.S., Lampe, P.D., and Johnson, R.G. (1996). Properties and regulation of gap junctional hemichannels in the plasma membranes of cultured cells. J. Cell Biol. *134*, 1019–1030.

Martin, P.E.M., George, C.H., Castro, C., Kendall, J.M., Capel, J., Campbell, A.K., Revilla, A., Barrio, L.C., Evans, H.W. (1998). Assembly of chimeric connexin-aequorin proteins into functional gap junction channels. J. Biol. Chem. *273*, 1719–1726.

Meyer, R.A., Laird, D.W., Revel, J.P., and Johnson, R.G. (1992). Inhibition of gap junction and adherens junction assembly by connexin and A-CAM antibodies. J. Cell Biol. *119*, 179–189.

Murray, S.A., Williams, S.Y., Dillard, C.Y., Narayanan, S.K., and McCauley, J. (1997). Relationship of cytoskeletal filaments to annular gap junction expression in human adrenal cortical tumor cells in culture. Exp. Cell Res. *234*, 398–404.

Musil, L.S., Cunningham, B.A., Edelman, G.M., and Goodenough, D.A. (1990). Differential phosphorylation of the gap junction protein connexin43 in junctional communication-competent and -deficient cell lines. J. Cell Biol. *111*, 2077–2088.

Musil, L.S., and Goodenough, D.A. (1991). Biochemical analysis of connexin43 intracellular transport, phosphorylation, and assembly into gap junctional plaques. J. Cell Biol. *115*, 1357–1374.

Naray-Fejes-Toth, A., and Fejes-Toth, G. (1996). Subcellular localization of the type 2 11-beta-hydroxysteroid dehydrogenase. A green fluorescent protein study. J. Biol. Chem. *271*, 15436–15442.

Naus, C.C., Hearn, S., Zhu, D., Nicholson, B.J., and Shivers, R.R. (1993). Ultrastructural analysis of gap junctions in C6 glioma cells transfected with connexin43 cDNA. Exp. Cell Res. *206*, 72–84.

Oberhauser, A.F., and Fernandez, J.M. (1995). Hydrophobic ions amplify the capacitive currents used to measure exocytotic fusion. Biophys. J. *69*, 451–459.

Ormo, M., Cubitt, A.B., Kallio, K., Gross, L.A., Tsien, R.Y., and Remington, S.J. (1996). Crystal structure of the *Aequorea victoria* green fluorescent protein. Science *273*, 1392–1395.

Pedraza, L., Fidler, L., Staugaitis, S.M., and Colman, D.R. (1997). The active transport of myelin basic protein into the nucleus suggests a regulatory role in myelination. Neuron *18*, 579–589.

Presley, J.F., Cole, N.B., Schroer, T.A., Hirschberg, K., Zaal, K.J., and Lippincott-Schwartz, J. (1997). ER-to-Golgi transport visualized in living cells. Nature *389*, 81–85.

Reaume, A.G., de Sousa, P.A., Kulkarni, S., Langille, B.L., Zhu, D., Davies, T.C., Juneja, S.C., Kidder, G.M., and Rossant, J. (1995). Cardiac malformation in neonatal mice lacking connexin43. Science *267*, 1831–1834.

Rup, D.M., Veenstra, R.D., Wang, H.Z., Brink, P.R., and Beyer, E.C. (1993). Chick connexin-56, a novel lens gap junction protein. Molecular cloning and functional expression. J. Biol. Chem. *268*, 706–712.

Severs, N.J., Shovel, K.S., Slade, A.M., Powell, T., Twist, V.W., and Green, C.R. (1989). Fate of gap junctions in isolated adult mammalian cardiomyocytes. Circ. Res. *65*, 22–42.

Simon, A.M., Goodenough, D.A., Li, E., and Paul, D.L. (1997). Female infertility in mice lacking connexin 37. Nature *385*, 525–529.

Sullivan, R., and Lo, C.W. (1995). Expression of a connexin 43/beta-galactosidase fusion protein inhibits gap junctional communication in NIH3T3 cells. J. Cell Biol. *130*, 419–429.

Traub, O., Look, J., Paul, D., and Willecke, K. (1987). Cyclic adenosine monophosphate stimulates biosynthesis and phosphorylation of the 26 kDa gap junction protein in cultured mouse hepatocytes. Eur. J. Cell Biol. *43*, 48–54.

Veenstra, R.D., Wang, H.Z., Westphale, E.M., and Beyer, E.C. (1992). Multiple connexins confer distinct regulatory and conductance properties of gap junctions in developing heart. Circ. Res. *71*, 1277–1283.

Wacker, I., Kaether, C., Kromer, A., Migala, A., Almers, W., and Gerdes, H.H. (1997). Microtubule-dependent transport of secretory vesicles visualized in real time with a GFP-tagged secretory protein. J. Cell Sci. *110*, 1453–1463.

Wang, H.G., Rapp, U.R., and Reed, J.C. (1996). Bcl-2 targets the protein kinase Raf-1 to mitochondria. Cell *87*, 629–638.

Wang, Y., and Rose, B. (1995). Clustering of Cx43 cell-to-cell channels into gap junction plaques: regulation by cAMP and microfilaments. J. Cell Sci. *108*, 3501–3508.

Wubbolts, R., Fernandez-Borja, M., Oomen, L., Verwoerd, D., Janssen, H., Calafat, J., Tulp, A., Dusseljee, S., and Neefjes, J. (1996). Direct vesicular transport of MHC class II molecules from lysosomal structures to the cell surface. J. Cell Biol. *135*, 611–622.

Yano, M., Kanazawa, M., Terada, K., Namchai, C., Yamaizumi, M., Hanson, B., Hoogenraad, N., and Mori, M. (1997). Visualization of mitochondrial protein import in cultured mammalian cells with green fluorescent protein and effects of overexpression of the human import receptor Tom20. J. Biol. Chem. *272*, 8459–8465.

Zampighi, G., Kreman, M., Ramon, F., Moreno, A.L., and Simon, S.A. (1988). Structural characteristics of gap junctions. I. Channel number in coupled and uncoupled conditions. J. Cell Biol. *106*, 1667–1678.